

# Linking decomposition rates of soil organic amendments to their chemical composition

J. A. Baldock <sup>A</sup>, C. Creamer<sup>A,B</sup>, S. Szarvas<sup>A</sup>, J. McGowan<sup>A</sup>, T. Carter<sup>A</sup>, and M. Farrell <sup>A,C</sup>

<sup>A</sup>CSIRO Agriculture and Food, Locked Bag 2, Glen Osmond, SA 5064, Australia.

<sup>B</sup>US Geological Survey, 345 Middlefield Road, Menlo Park, CA 94026, USA.

<sup>C</sup>Corresponding author. Email: mark.farrell@csiro.au

**Abstract.** The stock of organic carbon contained within a soil represents the balance between inputs and losses. Inputs are defined by the ability of vegetation to capture and retain carbon dioxide, effects that management practices have on the proportion of captured carbon that is added to soil and the application organic amendments. The proportion of organic amendment carbon retained is defined by its rate of mineralisation. In this study, the rate of carbon mineralisation from 85 different potential soil organic amendments (composts, manures, plant residues and biosolids) was quantified under controlled environmental conditions over a 547 day incubation period. The composition of each organic amendment was quantified using nuclear magnetic resonance and mid- and near-infrared spectroscopies. Cumulative mineralisation of organic carbon from the amendments was fitted to a two-pool exponential model. Multivariate chemometric algorithms were derived to allow the size of the fast and slow cycling pools of carbon to be predicted from the acquired spectroscopic data. However, the fast and slow decomposition rate constants could not be predicted suggesting that prediction of the residence time of organic amendment carbon in soil would likely require additional information related to soil type, environmental conditions, and management practices in use at the site of application.

**Keywords:** soil organic matter, SOM, spectroscopy, NMR, FTIR, residue, compost, manure, biosolid, mineralisation, chemometrics, PLSR.

Received 15 September 2020, accepted 14 January 2021, published online 11 February 2021

## Introduction

The amount of organic carbon (OC) contained within mineral soils is considered an important attribute with regards to both fertility and potential for carbon (C) sequestration. Measurements of soil OC content, stock or composition have been included as indicators of soil quality or soil health (e.g. Reeves 1997; Shukla *et al.* 2006; Manlay *et al.* 2007; Hoyle *et al.* 2011; de Freitas Maia *et al.* 2013). In addition to providing a positive contribution to a range of soil properties important to defining productivity and resilience, fluctuations in the content or stock of OC in soil also influence the magnitude of greenhouse gas emissions associated with agricultural practices. Changes to the stocks of OC found in soil will directly impact atmospheric concentrations of CO<sub>2</sub> (Baldock *et al.* 2012) and indirectly impact net emissions of nitrous oxide (N<sub>2</sub>O) by altering the balance of nitrogen (N) mineralisation and immobilisation and thus rates of nitrification and denitrification (Dalal *et al.* 2003; Hénault *et al.* 2012; Macdonald *et al.* 2016; Guenet *et al.* 2021).

The stock of OC in mineral soils results from the balance between the rates of OC input to and loss from soil. The magnitude of annual changes in soil organic carbon (SOC), expressed as a function changes in soil C stocks ( $\Delta$ SOC) can be represented using a mass balance approach according to Eqn 1

in which  $C_A$  is the rate of OC addition to soil and  $C_L$ ,  $C_E$  and  $C_M$  represent the respective rates of OC loss due to leaching, erosion and mineralisation with all values given in units of Mg C ha<sup>-1</sup> year<sup>-1</sup> (Baldock 2007).

$$\Delta SOC = C_A - C_L - C_E - C_M \quad (1)$$

Rates of addition of OC to soils in native ecosystems are defined by the net primary productivity (NPP) of the vegetation present and the proportion of that NPP that is added to soil. In most agricultural systems, NPP exerts primary control over inputs of OC. However, this can be modified substantially by management practices that affect root/shoot ratio, harvest index, retention and extent of incorporation of plant residues into soil and the application of organic amendments (OAs) (Paustian *et al.* 1997), particularly OAs derived from off-site waste streams (e.g. animal manures, biosolids, organic materials such as composts associated with recycling schemes). In addition to altering SOC stock, applying waste organic materials to soil may avoid, or at least reduce, potential emissions of methane associated with stockpiling or sending organic wastes to landfills.

Once added to a soil, subsequent increases in SOC stock can result directly from the retention of OA derived OC, or

indirectly though potential positive impacts on NPP. The retention of OA carbon (OAC) will be influenced by its subsequent rate of mineralisation and it is likely that any increases in SOC stocks will not be maintained without continued periodic additions of the amendment. Johnston *et al.* (2009) presented data derived from the Hoosfield Continuous Barley experiment showing that when annual farmyard manure applications of 35 Mg manure ha<sup>-1</sup> year<sup>-1</sup> for 19 years were suspended, the previous increase in SOC stock was lost over time and the SOC stocks approached but did not return completely to those present in the soil that had received no manure. Where manure application was maintained, a further increase in SOC stock towards a new equilibrium value occurred that was maintained.

The decomposition of SOC and OAC applied to soil typically follows a first-order exponential decay pattern (Paul and Clark 1996). Frequently, such decomposition patterns have two or more discrete phases which are reflective of a succession of soil processes including the direct mineralisation of OC from plant residues and any added OAC, and subsequent turnover of microbial products synthesised during the decomposition of these materials (Kalbitz *et al.* 2003; Adair *et al.* 2008; Glanville *et al.* 2016). A range of amendment, soil and environmental properties and processes will interact to define the rate, extent and partitioning of OAC mineralisation, including: (1) the inherent recalcitrance of the OA due to its biochemical composition, (2) the capability of organisms within the soil and amendment to degrade and use OAC, (3) the presence or absence of mechanisms of physical protection offered by soil minerals (adsorption onto mineral surfaces and burial within aggregations of mineral particles), and (4) fluctuations in environmental conditions (e.g. temperature and availability of oxygen, water and nutrients) (Baldock 2007).

Where OAs are added to soil to enhance SOC stocks through the retention of OAC, OAs that offer the greatest resistance to biological attack and therefore the lowest loss of OAC via respiration are desired. OAs have a wide range of chemical and biophysical characteristics that can influence the mineralisation and retention of OAC in soil (Thuriès *et al.* 2002). The susceptibility of OAs to decomposition, often referred to as the of maturity of the amendment in the context of composts, has been characterised by a range of approaches that quantify CO<sub>2</sub>-C emission either directly or via colourimetric approaches (e.g. the Solvita test; Rynk 2003). Other simple indices used to quantify the susceptibility to decomposition of natural organic materials include C/N ratio (e.g. Taylor *et al.* 1989) and lignin/N ratio (e.g. Melillo *et al.* 1982; Walela *et al.* 2014); however, consistent trends are not always observed (e.g. Bonanomi *et al.* 2013) potentially due to the progressive changes that occur in the biochemical composition of organic materials during decomposition. Such changes result from a selective utilisation of the more biologically labile components and a concomitant concentration of the more biologically recalcitrant components (Baldock *et al.* 1997, Bonanomi *et al.* 2013, Incerti *et al.* 2017). By assessing the relationship between OA biochemical composition and the susceptibility

of OAC to mineralisation, OAs that are most efficient at directly increasing and maintaining SOC stocks can be identified.

In this study, the rate of OAC mineralisation to CO<sub>2</sub> from a range of potential OAs was quantified and fitted to a two-pool exponential decay function to characterise their relative stabilities to biological decomposition. The composition of the organic amendments was characterised using solid-state nuclear magnetic resonance (NMR), mid-infrared (MIR) and near-infrared (NIR) spectroscopies. NMR was used to provide a robust assessment of the chemical composition of OAC and how that composition alters the susceptibility of the OACs to mineralisation. The traditional approach of dividing NMR spectra into chemical shift regions has been extended through the application of chemometric approaches to the entire NMR spectral range. MIR and NIR spectroscopies were included to assess the potential of developing a rapid and reliable spectroscopic method for defining the susceptibility of the OAs to decomposition and thus, their usefulness as a soil amendment designed to increase and maintain SOC stocks.

## Materials and methods

### *Organic amendments*

A total of 85 different potential OAs for soil including: 50 composts sourced from a range of composting facilities located around Australia, six manures derived from different animal species, 10 fresh plant residues derived from the major Australian crop species and some alternative species, and 19 biosolids obtained from a range of urban and rural wastewater plants. This variety of material was selected to provide a range of compositions and extents of decomposition indicative of organic materials that could potentially be added as amendments to soil. After collection, all materials were air-dried to constant mass at 40°C, finely ground (<50 µm) and mixed. Total C and total N contents of the air-dried and finely ground OAs were determined using a LECO TruMac (LECO Corporation, St Joseph, MI, USA) automated dry combustion analyser. Inorganic C contents were determined using method 19B of Rayment and Lyons (2011). Organic C contents were calculated as the difference between total C and inorganic C contents.

### *Incubation conditions*

A mass of each amendment equivalent to 0.4 g of OC was added to 22.7 g of a sand/soil/water mixture. The sand/soil/water mixture was prepared by mixing 2.7 kg of acid-washed sand (Cyclone dust, Sloans Sands, Dry Creek, SA) with 300 g of a soil inoculum and 400 g Milli-Q water on an aerated rotary mixer for two weeks. During the two-week mixing period, the weight of the sand/soil/water system was maintained by adding a required amount of Milli-Q water every 2–3 days. The soil inoculum was prepared by mixing 5 g of air-dry soil from the 0–10 cm layer of 200 different non-calcareous Australian agricultural soils collected as part of a national soil carbon research program (Baldock *et al.* 2013b) in order to capture diversity in soil microbiota from across Australia's agricultural soils. To prepare samples for incubation, the required masses

of the sand/soil/water mixture and an OA were placed into a PVC holder (50 mm high and 43 mm internal diameter) equipped with a 50  $\mu\text{m}$  mesh base. Four control samples without an OA added were also prepared in an identical manner and incubated alongside the OA-treated mixtures. The mixture was homogenised by mixing with a spatula and the surface was levelled. The prepared cores were immediately placed into sealed 226  $\text{cm}^3$  glass bottles containing a plastic vial with 10 mL of water and then incubated for 547 days. The water content of the incubated samples corresponded to 60% of the total water holding capacity measured after allowing saturated sand/soil to drain completely. This water content was controlled by regular weighing and addition of water as required to maintain the initial sample mass. No additional nutrients were added to the incubation system beyond those present in the OAs as they were collected.

We quantified of  $\text{CO}_2$  evolution from the samples periodically over 547 days (0, 4, 6, 11, 19, 26, 34, 48, 64, 103, 153, 204, 243, 306, 376, 432, 498 and 547 days). At the start of each incubation period (e.g. days 4–11) the headspace in the bottles containing incubating samples was refreshed by opening the bottles and allowing them to equilibrate with the atmosphere of the incubation room. The bottles were then closed, and a 2 mL sample of the headspace was immediately extracted and analysed by infrared gas analyser (Li-Cor Li-820, LI-COR Biosciences, Lincoln, NE, USA) and a circulation pump (Sanderman *et al.* 2017). The samples were then left to incubate in their closed bottles for the specified period after which time a second 2 mL sample of the headspace was extracted and analysed. The bottles were then opened to allow equilibration with the room atmosphere and the cycle was repeated for the next incubation period. Values from the start of each incubation period were subtracted from those at the end to ensure that only the  $\text{CO}_2$  evolved during each time point was counted.

The amendments accounted for 93.5% of the total OC present in the incubated samples. After 547 days of incubation, the cumulative  $\text{CO}_2\text{-C}$  emitted from the control samples was  $32.9 \pm 21.8$  mg C (average  $\pm$  standard deviation) accounting for  $12.3 \pm 5.4\%$  of the total  $\text{CO}_2\text{-C}$  emitted from the samples. The mean  $\text{CO}_2$  values from the control samples were subtracted from the OA-treated samples at each time point.

#### Modelling $\text{CO}_2\text{-C}$ emissions

Cumulative  $\text{CO}_2\text{-C}$  emissions over the 547 day incubation were calculated for each sample by summing the  $\text{CO}_2\text{-C}$  emitted (expressed in  $\text{mg CO}_2\text{-C g}^{-1}$  amendment carbon) during each successive incubation period. A two-pool first order exponential decay model (Eqn 2) was then fitted to the cumulative  $\text{CO}_2\text{-C}$  emission data ( $C_{\text{min}}$ ) collected through time ( $t$ ) by minimising the sum of squares of differences between measured and modelled values through an iterative adjustment of the size of the fast decomposing pool ( $C_f$ ), the decomposition rate constant for the fast pool ( $f$ ) and the decomposition rate constant for the slow pool ( $s$ ). The size of the slow decomposing pool ( $C_s$ ) was not iteratively fitted, but rather set to a value  $1000 - C_f$  since our objective was to

examine the relationship between mineralisability and chemical composition of all OC present in the various amendments.

$$C_{\text{min}} = C_f(1 - e^{-ft}) + C_s(1 - e^{-st}) \quad (2)$$

This fitting process was completed using the GRG Nonlinear solving method of the Solver add-on in Microsoft Excel 2013 with the default options other than the values assigned to the constraint precision and convergence values which were set to  $10^{-10}$ . The constraints imposed on the fitting process included:  $f \leq s$ ,  $f$  and  $s$  had to be  $\leq 1$  and  $\geq 0$  and  $C_f \leq 1000$ . Initial estimates of the values of  $C_f$ ,  $f$ , and  $s$  were calculated according to Eqns 3–5 where  $\text{CO}_2\text{-C}_i$  was the array of measured cumulative  $\text{CO}_2\text{-C}$  values obtained for a sample and  $T_i$  was the array of incubation durations. The value of  $C_s$  was calculated from the fitted value of  $C_f$  according to Eqn 6. Varying the magnitude of the initial estimates of  $C_f$ ,  $f$ , and  $s$  by  $\pm 5\%$ ,  $\pm 10\%$  or  $\pm 20\%$  did not alter the optimal solution obtained by the solver.

$$C_f = \text{Median}(\text{CO}_2 - C_i) \quad (3)$$

$$f = -\ln\left(\frac{\frac{\text{Median}(\text{CO}_2 - C_i)}{1000}}{\text{Median}(T_i)}\right) \quad (4)$$

$$s = -\text{LN}\left(1 - \frac{\frac{1000 - \text{Median}(\text{CO}_2 - C_i)}{1000}}{\text{Max}(T_i)}\right) \quad (5)$$

$$C_s = 1000 - C_f \quad (6)$$

#### Spectroscopic analyses

##### NMR spectroscopy

Solid-state  $^{13}\text{C}$  NMR analyses were completed on a Bruker 200 Avance spectrometer equipped with a 4.7 T wide-bore superconducting magnet operating at a resonance frequency of 50.33 MHz. Weighed samples (150–600 mg) were packed into 7 mm diameter zirconia rotors with Kel-F end caps and spun at 5 kHz. All analyses were completed using full rotors. Only one replicate of each finely ground organic amendment was analysed by NMR. Chemical shift values were calibrated to the methyl resonance of hexamethylbenzene at 17.36 ppm and a 50 Hz Lorentzian line broadening was applied to all spectra.

Three separate  $^{13}\text{C}$  NMR experiments were performed. An inversion recovery pulse sequence using eight inversion recovery times varying from 0.001 to 3.0 s and a recycle delay ( $d_1$ ) between pulses, varying from 5 to 15 s, was applied to each amendment. The array and recycle delay values used for each amendment were varied to optimise the calculation of the spin-lattice relaxation time ( $T_{1H}$ ). The  $T_{1H}$  values were used to define amendment specific values for recycle delays in the subsequent cross polarisation (CP)  $^{13}\text{C}$  NMR analyses. In the CP analyses the recycle delay was set to the longer of 1 s or five times  $T_{1H}$  to ensure that acquired signal intensities were not influenced by saturation. Subsequent CP analyses used a 3.2  $\mu\text{s}$ , 195 w,  $90^\circ$  pulse, a contact time of 1 ms and a recycle delay derived from the  $T_{1H}$  analysis (1–5 s). Between 2000 and 15 000 scans were collected for each CP analysis. The number of scans was increased as the amount of C contained in

the rotor declined across the various amendments. A variable spin lock experiment using an array of spin lock times (1, 2, 6, 10, 15, 20 ms), a contact time of 1 ms and a recycle delay of 1 s was performed to calculate amendment specific  $T_{1\rho}H$  values and allow the CP NMR observability of OC in the amendments to be quantified as described by Baldock and Smernik (2002) using glycine as an external signal intensity standard.

All spectral processing including the calculation of  $T_1H$  and  $T_{1\rho}H$  and integration of spectral regions was completed using the Bruker TopSpin 3.2 software. After phasing and baseline corrections were applied, the absolute NMR signal intensities acquired for each sample were divided by the number of scans collected and corrected for empty rotor background signals. The resultant NMR spectra were normalised by dividing the intensity at each chemical shift value by the total intensity acquired over the entire spectrum (350–100 ppm). The normalised spectra were integrated to allocate the total signal intensity acquired to the chemical shift regions described by Baldock *et al.* (2013b). Additionally, the normalised spectra in their entirety were used directly in chemometric analyses.

#### *MIR and NIR spectroscopy*

MIR and NIR spectroscopic analyses were completed on a single replicate of each finely ground OA using a Nicolet 6700 FTIR spectrometer (Thermo Fisher Scientific Inc., MA, USA) equipped with a Pike AutoDiff-Automated diffuse reflectance accessory (Pike Technologies, WI, USA). Samples (~100 mg) were packed into stainless steel cups and the surface levelled before being loaded into the 60 position wheel associated with the Pike AutoDiff. MIR spectra were acquired over 8000–400  $\text{cm}^{-1}$  with a resolution of 8  $\text{cm}^{-1}$  using a KBr beam-splitter and a deuterated triglycine sulphate (DTGS) detector (Thermo Fisher Scientific Inc.). NIR spectra were acquired over 10000–4000  $\text{cm}^{-1}$  with a resolution of 8  $\text{cm}^{-1}$  using a quartz beam-splitter and a thermo-electrically cooled (TE) indium gallium arsenide (InGaAs) detector (Thermo Fisher Scientific Inc.). For both MIR and NIR analyses, the background signal intensity was quantified by collecting 240 scans on a silicon carbide disk before analysing each set of 60 soil samples and used to correct the signal obtained for the soil samples. A total of 60 scans were acquired and averaged to produce MIR and NIR reflectance spectra for each individual sample and the Omnic software (Version 8.0; Thermo Fisher Scientific Inc., MA, USA) was used to convert the acquired reflectance spectra into absorbance spectra (log-transform of the inverse of reflectance).

#### *Correlation and chemometric analyses*

Pearson correlation between the parameters derived by fitting the two-pool decomposition model ( $C_f$ ,  $f$ ,  $C_s$  and  $s$ ), total amount of  $\text{CO}_2\text{-C}$  respired, OC and total N contents, C/N ratio and the allocation of NMR signal intensity to the chemical shift regions were defined using the *R* statistical environment version 4.03 (R Core Team 2020). Initial data cleaning was conducted using the ‘tidyverse’ package suite (Wickham *et al.* 2019) before construction of the correlogram using the ‘corrplot’ package (Wei and Simko 2017).

All chemometric analyses including data transformations, principal components analysis (PCA) and partial least-squares regression (PLSR) performed on the acquired spectra (NMR, MIR and NIR) and analytical data were completed using Unscrambler 10.3 (CAMO Software, Oslo, Norway). Prior to chemometric analyses, the MIR spectra were truncated to a spectral range of 6000–600  $\text{cm}^{-1}$  and a baseline offset transformation was applied. The NIR spectra were truncated to 8000–4000  $\text{cm}^{-1}$  and a baseline offset followed by a second order polynomial de-trending algorithm were applied to transform the spectra before applying any chemometric analyses. No further preprocessing of the NMR spectra was applied. All spectral data was mean centred by the Unscrambler software before initiating PCA and PLSR analyses.

PCA was used to assess the variability of the transformed NMR, MIR and NIR spectra acquired for the 85 OAs. The PCAs used the spectra acquired from all 85 amendments and were completed using a full cross validation. PLSR was used to assess whether predictive algorithms for the parameters of the two-pool first order exponential decay model ( $C_f$ ,  $f$ ,  $C_s$  and  $s$ ) could be derived from the NMR, MIR or NIR spectra. The approach taken to perform all PLSR analyses included the following series of steps. A PLSR model was constructed using full cross validation. The Kennard Stone algorithm was then applied to identify 50 of the 85 amendments that best accounted for the variability in the model parameter being predicted and the spectral data. These 50 samples were then defined as a calibration set and the remaining 35 amendments were defined as an independent validation set. The PLSR was then repeated using a test set validation approach. The quality of the derived models (PCA and PLSR) was assessed using a range of statistics including  $R^2$  (the proportion of total variance of the residuals explained), root mean square error (RMSE), standard error of prediction (SEP) and bias as presented in Baldock *et al.* (2013a).

#### *Data availability*

All data collected in this study for the organic amendments including elemental composition, temporal amounts of OAC mineralised and acquired NMR, MIR and NIR spectra are available in the CSIRO Data Access Portal (Farrell *et al.* 2021).

## Results

### *Elemental contents of organic amendments*

Organic C contents of the OAs included in this study ranged from 44 to 439  $\text{g OC kg}^{-1}$  OA with a mean and standard deviation of 280  $\text{g OC kg}^{-1}$  OA and 101  $\text{g OC kg}^{-1}$  OA, respectively. Total N contents ranged from 3 to 72  $\text{g N kg}^{-1}$  OA with a mean and standard deviation of 22  $\text{g N kg}^{-1}$  OA and 17  $\text{g N kg}^{-1}$  OA, respectively. The variation in OC and TN contents led to a wide range of C/N ratios (5–142  $\text{g OC g}^{-1}$  N) with an average of 22  $\text{g OC g}^{-1}$  N and a standard deviation of 27  $\text{g OC g}^{-1}$  N. The corresponding values for each class of OA are provided in Table 1. These results demonstrate the diverse nature of the OAs used to assess the impact of chemical composition on rates of decomposition.

**Table 1.** Mean, standard deviation of the mean, and median organic carbon and total nitrogen contents of the four classes of soil organic amendments

Parameter	Type of organic amendment	Count	Minimum	Maximum	Median	Mean	Standard deviation
Organic carbon content (g OC kg <sup>-1</sup> organic amendment)							
	Compost	54	71	434	248	243	78
	Manures	5	364	409	377	382	20
	Plant residues	10	411	439	424	425	9
	Biosolids	20	44	420	309	281	112
Total nitrogen content (g N kg <sup>-1</sup> organic amendment)							
	Compost	54	4	50	15	16	8
	Plant residues	5	16	44	23	26	12
	Manures	10	3	23	7	9	6
	Biosolids	20	4	72	46	43	20
C/N ratio (g organic carbon/g total nitrogen)							
	Compost	54	5	92	14	18	15
	Plant residues	5	8	24	16	17	7
	Manures	10	18	142	57	74	45
	Biosolids	20	5	11	6	7	2

### Mineralisation of amendment organic carbon

Total CO<sub>2</sub>-C emission over the 547 day incubation period from the OAs varied from 68 to 516 mg CO<sub>2</sub>-C g<sup>-1</sup> OAC with a mean of 251 and a standard deviation of 105 mg CO<sub>2</sub>-C g<sup>-1</sup> OAC (Fig. 1). The compost and biosolids tended to emit less CO<sub>2</sub>-C than the plant residues or manures, consistent with their potentially greater extent of decomposition. The greatest variance in CO<sub>2</sub>-C emission within the individual classes of OA occurred within the composts and plant residues, with manures showing the lowest variance. Given that the purpose of this study was to link OAC chemical composition to mineralisation, large differences in CO<sub>2</sub>-C emission across the amendments were desirable and indicated that an appropriate set of OAs were included in the study.

The temporal patterns of CO<sub>2</sub>-C emission obtained over the entire 547 day incubation are shown in Fig. 2 from single OAs exhibiting a high (Fig. 2a) and a low (Fig. 2c) CO<sub>2</sub>-C emission. When the CO<sub>2</sub>-C emission data derived from each amendment were fitted to a two-pool exponential model (Eqn 2), a strong correspondence between measured and modelled values was obtained for all 85 OAs. For five of the amendments, the predicted values obtained for the decomposition rate constants of the fast and slow pools were equivalent, indicating that the measured data could be adequately described by a one-pool exponential model. For the five amendments where this occurred, the magnitudes of the one-pool decomposition rate constants were consistent with the slow pool of all other amendments where CO<sub>2</sub>-C emission was better described by the two-pool model. This result suggested that five amendments did not contain a fast pool and therefore, the OC contained within these five amendments was allocated entirely to the slow pool for all subsequent analyses.

Examples of the partitioning of CO<sub>2</sub>-C emission to the modelled fast and slow pools is presented in Fig. 2a and c. Although temporal changes in the slow pool appeared linear, projecting the CO<sub>2</sub>-C emission beyond the 547 day incubation period (Fig. 2b and d) confirmed the exponential shape of the relationship and indicated that >15 years would be required

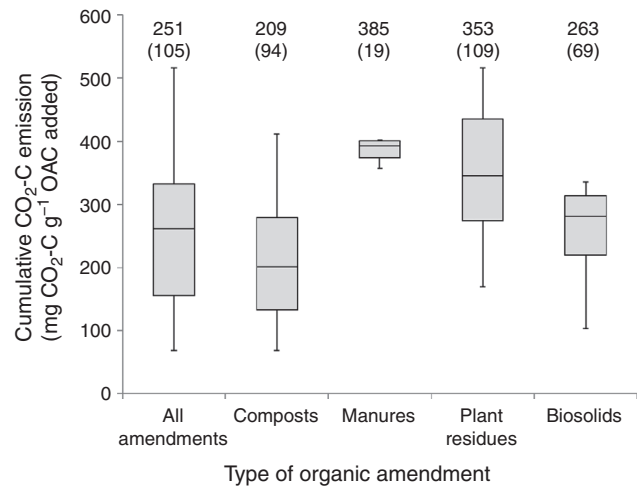


**Fig. 1.** Box plots showing the minimum, 25th percentile, median, 75th percentile and maximum total CO<sub>2</sub>-C emissions measured for 547 days from all amendments and from each class of amendment. Values above each box plot show the mean and standard deviation (in parentheses) associated with the amendments included in each box plot.

for the added amendment carbon to approach complete mineralisation provided that the temporal trends of CO<sub>2</sub>-C emission observed within the incubation period persisted.

The range and distribution of values obtained for each parameter included in the two-pool model across all amendments and for each type of amendment are presented in Fig. 3. For all amendments, the majority of C (>70%) was allocated to the slow C<sub>s</sub> pool with an average, standard deviation and range of 87%, 7% and 72–100%, respectively. The size of C<sub>s</sub> was greater in the composts and biosolids than in the manures and plant residues, although some overlap of the ranges of C<sub>s</sub> values did exist. The decomposition constants associated with the fast pool ranged from 3.6 × 10<sup>-4</sup> to 1.6 × 10<sup>-1</sup> days<sup>-1</sup> while those from the slow pool were on average two orders of magnitude smaller and ranged from 3.5 × 10<sup>-6</sup> to 7.8 × 10<sup>-4</sup> days<sup>-1</sup>.

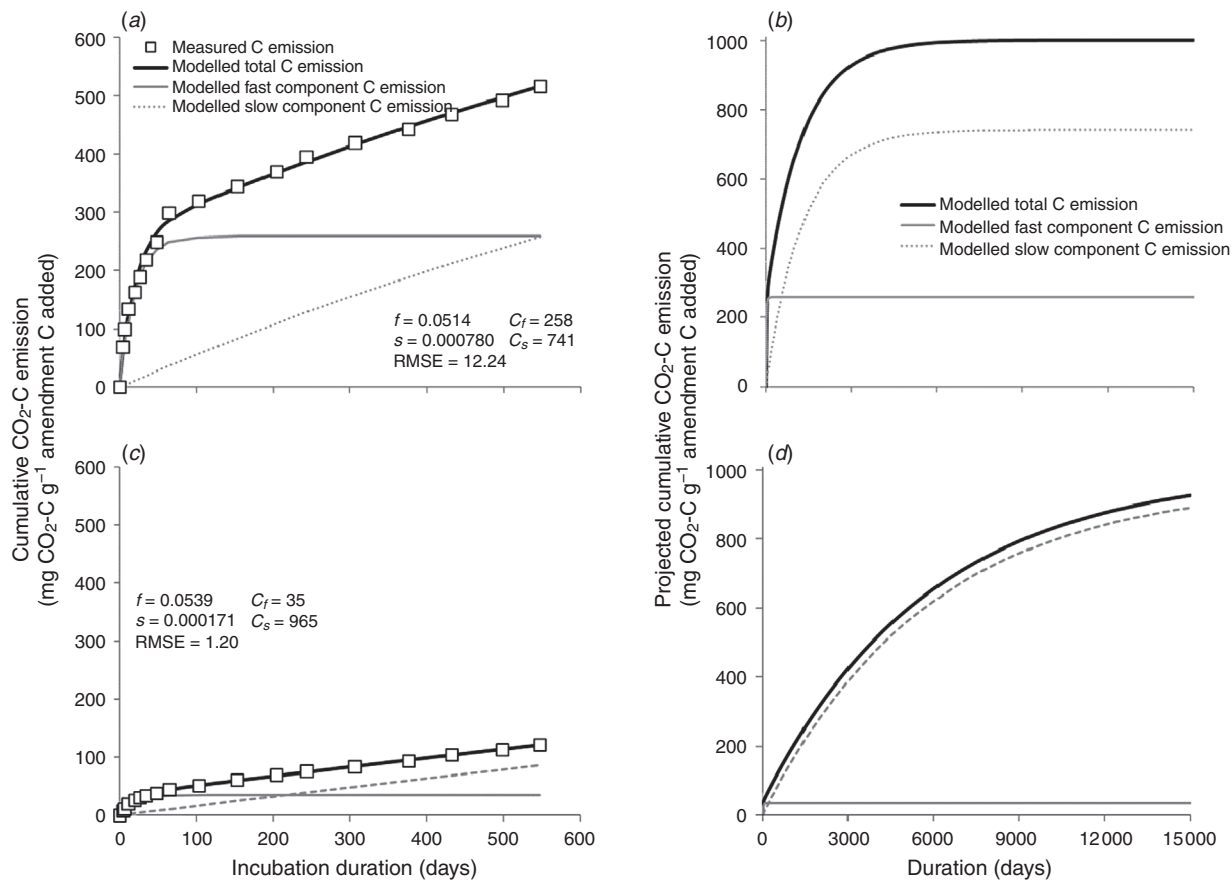


**Fig. 2.** Measured and modelled cumulative CO<sub>2</sub>-C emission from organic amendments exhibiting high (a) and low (c) CO<sub>2</sub>-C emission over the duration of the incubation. Projected cumulative mineralisation beyond the incubation duration derived for the same high (b) and low (d) CO<sub>2</sub>-C emitting amendments.

### NMR spectroscopic analyses

The <sup>13</sup>C NMR spectra acquired for all amendments exhibited resonances typical of those observed for fresh plant residues through to materials characterised by extensive decomposition. The average signal intensity across all 85 organic amendments for each chemical shift value (solid black line) as well as the minimum and maximum signal intensity obtained for each chemical shift value (dotted black lines) are presented in Fig. 4a. Each of the lines in Fig. 4a do not represent a real spectrum, but rather indicate the range and mean spectral intensities obtained at a given chemical shift value. The largest variations in spectral intensity occurred within the alkyl (0–45 ppm), O- and di-O-alkyl (60–110 ppm), and carbonyl (160–190 ppm) regions. Variation in the intensity allocated to aryl (110–145 ppm) and O-aryl C (145–165 ppm) was present but was of a lesser magnitude than that noted for the other forms of C.

PCA of the acquired <sup>13</sup>C NMR spectra showed a clustering by amendment type (Fig. 4b). PC-1 accounted for 85% of the NMR spectral variance. The loading spectrum generated for PC-1 (Fig. 4c) indicated that positive scores were associated with signals typical of carbohydrates and negative scores were associated signals typical of protein (see inset in Fig. 4c).

Decreases in carbohydrate C (particularly cellulose) and increases in protein C are often associated with increasing extent of decomposition (Baldock *et al.* 1997). PC-2 accounted for 10% of the NMR spectral variance with positive scores being associated with increased aryl and O-aryl C typical of lignin and negative scores being associated with increases in protein, carbohydrate and alkyl C (Fig. 4c). In response to these differences in PC loadings, the plant residues, representing the least decomposed material, had high PC-1 scores and low PC-2 scores. The manures fell in an intermediate position along PC-1 between the plant residues and more decomposed biosolid materials with some of the biosolids obtaining positive PC-2 scores. The composts spanned the largest range covering the majority of the range of PC-1 scores but tended to have higher contents of aryl and O-aryl C consistent with a relative accumulation of lignin during decomposition of the plant materials and green wastes from which they were derived.

### MIR and NIR spectroscopic analyses

Contrary to NMR, which only detects and differentiates forms of C in the amendments, MIR and NIR detect all chemical structures capable of absorbing infrared radiation, including

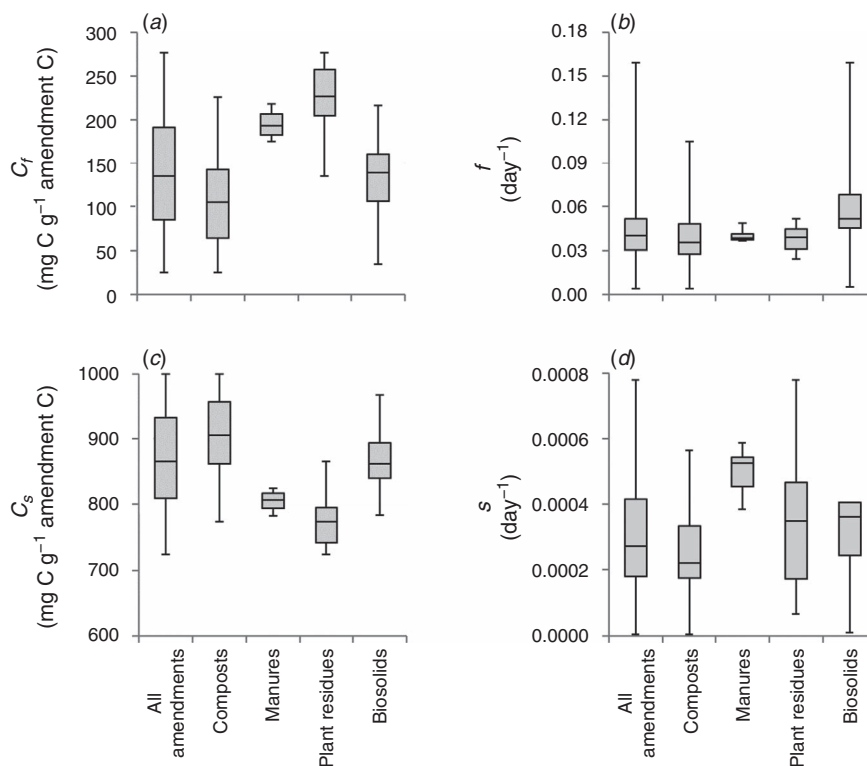


**Fig. 3.** Box plots showing the minimum, 25th percentile, median, 75th percentile and maximum values obtained for the parameters of the two-pool exponential decay model (Eqn 2) fitted to the measured CO<sub>2</sub>-C emission data across all amendments and for those associated with each type of amendment: (a) size of the fast pool ( $C_f$ ), (b) decomposition rate constant of the fast pool ( $f$ ), (c) size of the slow pool ( $C_s$ ) and (d) decomposition rate constant of the slow pool ( $s$ ).

mineral components. The presence of mineral components can therefore impact on spectral interpretations pertaining to the organic components due to an overlapping of signals.

The different amendments displayed a wide range of signal intensities over the 3800–600 cm<sup>-1</sup> region of the MIR spectra and the 7200–4000 cm<sup>-1</sup> region of the NIR spectra supporting a diversity of chemical composition across the amendments (Fig. 5a and Fig. 6a). As noted for the NMR spectra, the amendments tended to group together according to their type (compost, manure, plant residue, biosolid) in the PCA scores plots derived from the MIR and NIR data (Fig. 5b and Fig. 6b). However, the extent of separation of amendment types was not as strong as noted for the NMR spectra, particularly for the NIR spectra. Although not as definitive as noted for the NMR PCA, the features of the loading spectra obtained for PC-1 of the MIR spectra most closely resembles the inverse of a spectrum collected for cellulose (see inset to Fig. 5c) suggesting that carbohydrate content increases with decreasing PC-1 score. The two sharp signals near 1680 and 1540 cm<sup>-1</sup> in the loading spectrum of PC-2 may be indicative of amide groups in protein and the general shape of the positive values most closely resemble the MIR spectrum acquired for lignin. An increasing PC-2 score could therefore be associated with increasing contributions from protein and lignin. Both of these suggestions are consistent with the interpretation of the PCA loading spectra derived for the

NMR spectra, reflecting an increasing state of decomposition from plant residues with high carbohydrates and low protein, to manures with high carbohydrates and intermediate protein, and then to biosolids with high proteins (and composts with varying levels of protein and carbohydrates).

The loadings spectrum for PC-1 of the NIR spectra (Fig. 6c) resembled the inverse of the spectrum acquired for cellulose (see inset to Fig. 6c) indicating that carbohydrate content increased with decreasing PC-1 scores. This result is consistent with undecomposed plant residue samples being associated with negative PC-1 scores and a progression towards more positive PC-1 scores in progressing from the manure through to biosolid derived amendments. Composts tended to span across all PC-1 values indicative of their large diversity in composition. PC-2 scores could best be explained by a combination of the NIR spectra obtained for lignin and protein with contents increasing with increasing PC-2 score. As for the MIR analyses, these results are consistent with differences in the extent of decomposition across the OAs indicated by the NMR spectra.

#### Predicting mineralisation of OAC

Significant correlations ( $\alpha \leq 0.05$ ) were observed between the parameters describing OAC mineralisation over the incubation period (total mineralisation,  $C_f$ ,  $f$ ,  $C_s$ , and  $s$ ) and elemental

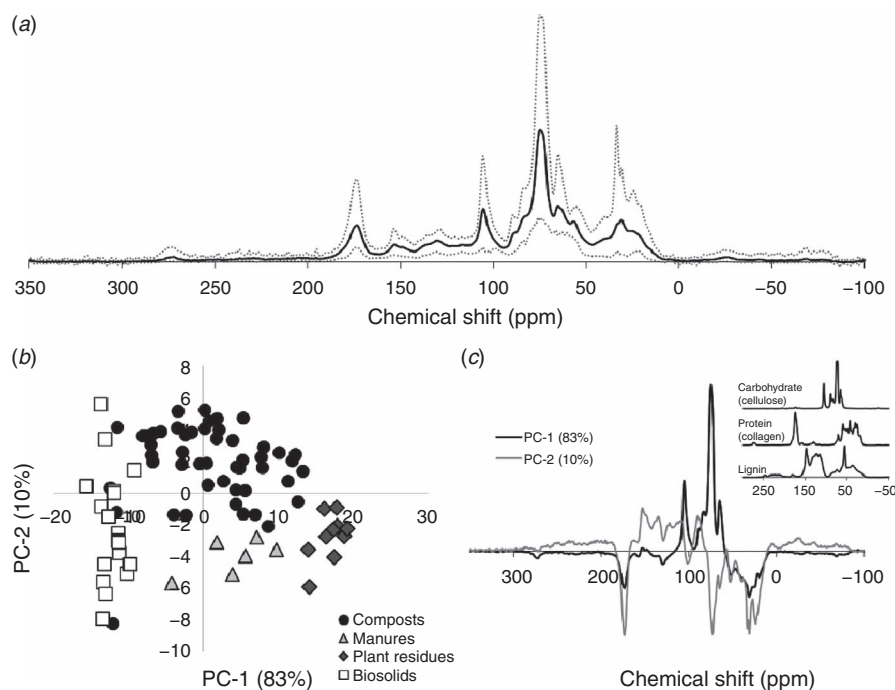


**Fig. 4.** (a) Average (solid line), minimum and maximum (dotted lines)  $^{13}\text{C}$  NMR signal intensities observed at each chemical shift value across all amendments. (b) Scores plot derived from a PCA applied to the NMR spectra (values in parenthesis represent the proportion of spectral variance explained by each principal component). (c) Loading spectra derived for PC-1 and PC-2 with an inset showing  $^{13}\text{C}$  NMR spectra of carbohydrate, protein and lignin.

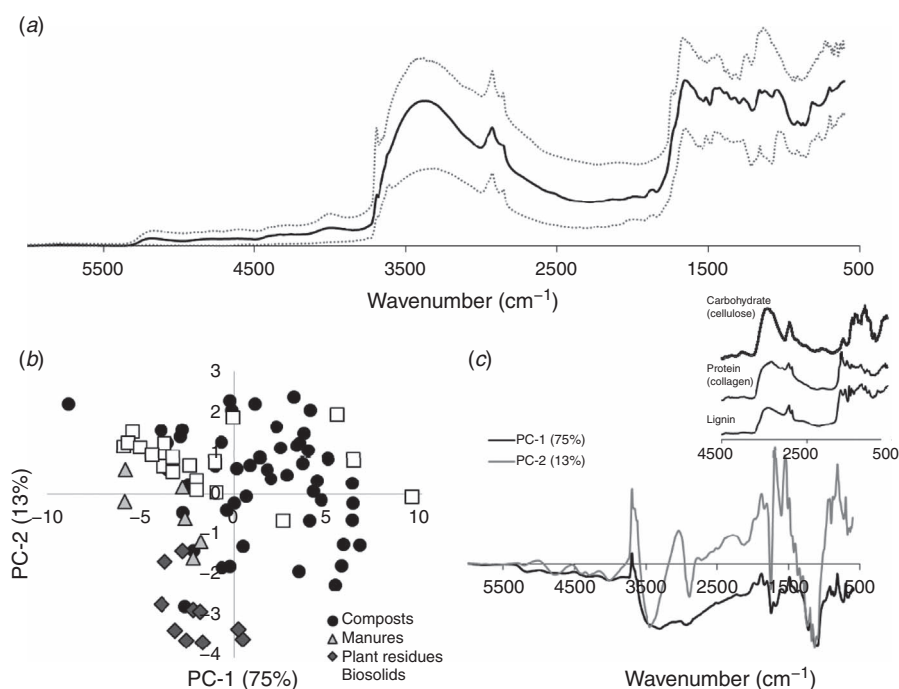


**Fig. 5.** (a) Average (solid line), minimum and maximum (dotted lines) diffuse reflectance MIR signal intensities observed at each wavenumber across all amendments. (b) Scores plot derived from a PCA applied to the MIR spectra (values in parenthesis represent the proportion of spectral variance explained by each principal component). (c) Loading spectra derived for PC-1 and PC-2 with an inset showing MIR spectra of carbohydrate, protein and lignin.

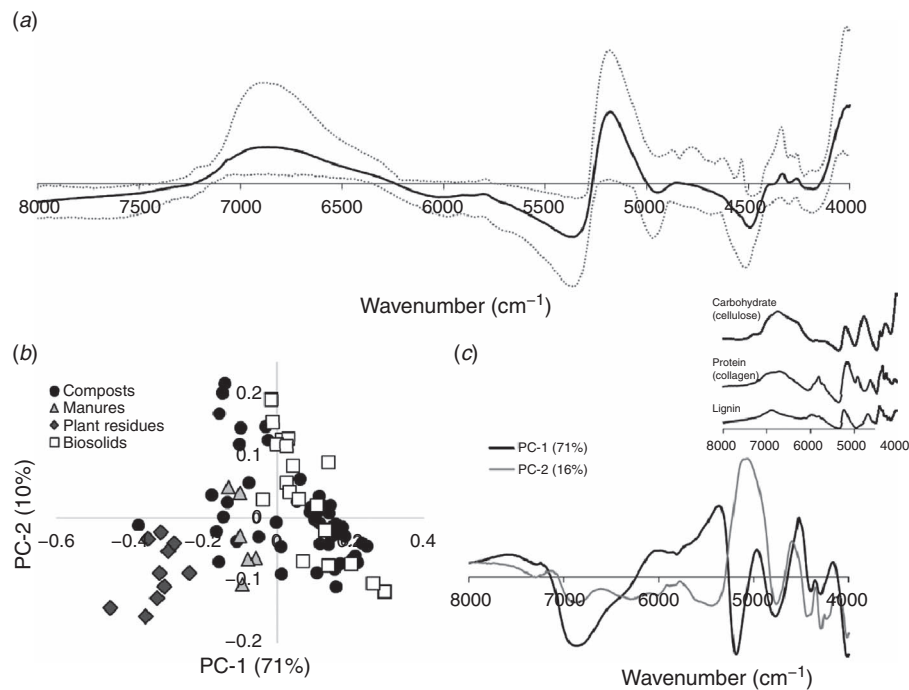


**Fig. 6.** (a) Average (solid line), minimum and maximum (dotted lines) NIR signal intensities observed at each wavenumber across all amendments. (b) Scores plot derived from a PCA applied to the NIR spectra (values in parenthesis represent the proportion of spectral variance explained by each principal component). (c) Loading spectra derived for PC-1 and PC-2 with an inset showing NIR spectra of carbohydrate, protein and lignin.

contents of the OAs (Supplementary Fig. S1). Total respiration was positively correlated with OC content ( $r = 0.67$ ) but a correlation with N content or C/N ratio was not observed.  $C_f$ ,  $C_s$ , and  $s$  were correlated with OC content ( $r = 0.69$ ,  $r = -0.69$  and  $r = 0.44$ , respectively), but not with N content or C/N ratio. However, a positive correlation between N content and  $f$  was observed ( $r = 0.45$ ).

Various positive and negative correlations were noted between the C mineralisation parameters and the allocations of total NMR signal intensity to the chemical shift regions (Supplementary Fig. S1).  $C_f$  was positively correlated with the proportion of NMR signal intensity allocated to the O-alkyl and alkyl regions ( $r = 0.51$  and  $F = 0.37$ , respectively) and negatively correlated with the allocation of signal to the aryl, O-aryl and ketone regions ( $r = -0.80$ ,  $r = -0.77$ , and  $r = -0.70$ , respectively). Given that the sum of the amounts of C allocated to the fast and slow pools was forced to sum to 1000 mg, the correlations obtained for  $C_s$  were the inverse of those found for  $C_f$ . Positive correlations were observed between  $f$  and allocations of NMR signal to the alkyl, N-alkyl and carbonyl regions ( $r = 0.45$ ,  $r = 0.32$ , and  $r = 0.46$ , respectively) while negative correlations were observed with allocations to the O-alkyl and di-O-alkyl regions ( $r = -0.33$  and  $-0.39$ ). For the decomposition constant of the slow pool ( $s$ ), negative correlations were noted with the allocation of NMR signal to the aryl, O-aryl and ketone regions ( $r = -0.45$ ,  $r = -0.51$ , and  $r = -0.36$ , respectively).

The ability of the acquired spectroscopic data to predict CO<sub>2</sub>-C emission from the various OAs was also assessed

through PLSR. If the chemical composition of the amendments as defined by the acquired NMR, MIR and NIR spectra influenced the magnitude and dynamics of CO<sub>2</sub>-C emission, it should be possible to develop PLSR algorithms capable of predicting the magnitude of the four parameters ( $C_f$ ,  $f$ ,  $C_s$ , and  $s$ ) used to model the measured CO<sub>2</sub>-C emissions. Additionally, the  $\beta$ -coefficients derived from PLSR prediction algorithms can be used to identify the spectral information, and thus the forms of C, important to defining any predictive capability realised.

The PLSR predictive algorithms and associated  $\beta$ -coefficients derived using the NMR spectra to predict  $C_f$ ,  $f$ ,  $C_s$  and  $s$  are presented in Fig. 7. The PLSR predictive algorithms explained 82% of the variation in  $C_f$  for the calibration amendments and 75% of the variation for the validation amendments with RMS and RMSEP values of 32.0 and 33.1 mg C<sub>f</sub>-C g<sup>-1</sup> OAC, respectively (Fig. 7a). The  $\beta$ -coefficients plot (Fig. 7b) indicated that increases in NMR signal intensity consistent with carbohydrate and protein structures increased the allocation of amendment carbon to  $C_f$  while increased signal intensity indicative of lignin structures reduced the allocation to  $C_f$ . The absolute values of the  $\beta$ -coefficients were inversely proportional to the strength of the concomitant signals noted in the acquired NMR spectra. Therefore, it is important to recognise that the presence of large  $\beta$ -coefficients is not necessarily indicative of regions in the original NMR spectra where substantial differences in signal intensity exist. This was exemplified by the smaller range of signal intensity associated with lignin structures in the

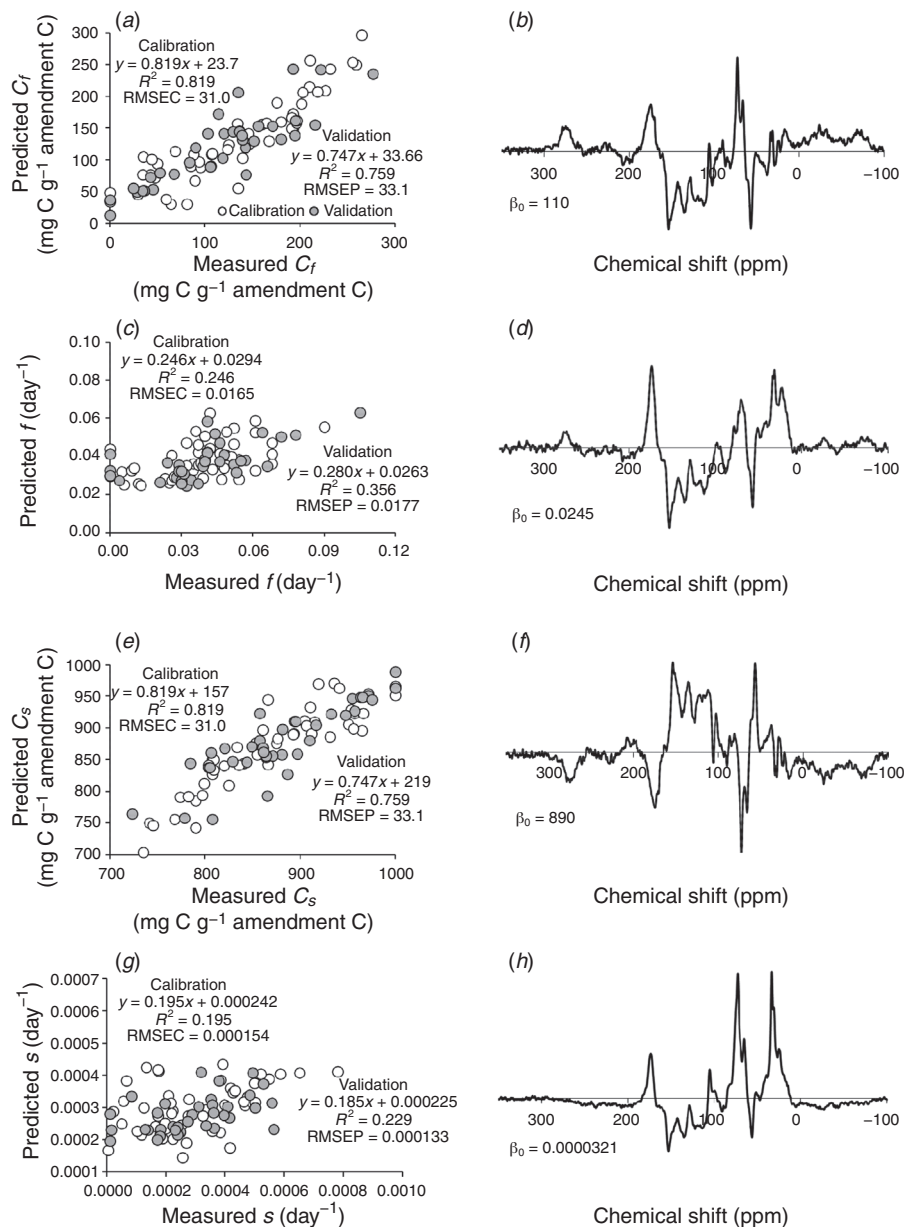


**Fig. 7.** Relationship between measured and predicted values of  $C_f$ ,  $f$ ,  $C_s$  and  $s$  (a, c, e and g, respectively) and the corresponding prediction algorithms developed from the NMR spectra (b, d, f and h, respectively).

original spectra (Fig. 4a) relative to that associated with carbohydrate structures.

Given that the value of  $C_s$  was derived as the difference between 1000 and  $C_f$ , the statistics associated with the calibration and validation PLSR algorithms for  $C_s$  (Fig. 7e) were the same as those obtained for  $C_f$ . Additionally, the  $\beta$ -coefficient plot (Fig. 7f) was a direct inverse of that obtained for  $C_f$ . For the decomposition rate constants  $f$  and  $s$ , only weak predictive relationships were obtained (Fig. 7c and e) from the application of PLSR analyses to the NMR spectra. However, variations in the magnitude of the  $\beta$ -coefficients suggested that both rate constants were increased by the presence of OC with NMR signal intensity consistent with

proteins and carbohydrates and reduced signal intensity consistent with lignin. These results demonstrated that the chemical composition of the amendments as defined by the acquired NMR spectra could be useful in defining the allocation of amendment carbon to the fast and slow decomposing pools based on the presence of signal intensity associated with carbohydrate, protein and lignin structures.

The PLSR predictive algorithms derived from the MIR and NIR spectra provided similar results to those obtained from NMR spectra with the exception of a reduction in predictive capacity (lower  $R^2$  values and increased RMS and RMSEP values) for the prediction of the allocation of amendment carbon to  $C_f$  and  $C_s$  (Table 2). Variations in the magnitude

**Table 2.** Statistics obtained for the PLSR algorithms derived from MIR and NIR spectra to predict the parameters of the two-pool exponential decomposition model

PLSR statistic	Sample set	MIR spectra				NIR spectra			
		$C_f$	$f$	$C_s$	$s$	$C_f$	$f$	$C_s$	$s$
Slope	Cal	0.749	0.451	0.749	0.790	0.757	0.361	0.757	0.359
	Val	0.693	0.283	0.693	0.373	0.593	0.238	0.593	0.36
Intercept	Cal	30.2	0.0215	30.2	0.0000659	33.8	0.0287	33.8	0.00022
	Val	43.8	0.0303	43.8	0.000188	47.1	0.0298	47.1	0.000207
RMSE	Cal	37.1	0.0168	37.1	0.0000775	35.4	0.0218	35.4	0.000129
	Val	37.8	0.0159	37.8	0.000142	36.4	0.0155	36.4	0.000126
$R^2$	Cal	0.749	0.451	0.749	0.790	0.757	0.361	0.757	0.359
	Val	0.666	0.114	0.666	0.193	0.743	0.326	0.743	0.529

of the  $\beta$ -coefficients associated with the MIR and NIR PLSR prediction algorithms were also consistent with those derived from NMR spectra. Increases in  $C_f$  were associated with a greater presence of carbohydrate and protein structures and a lower presence of lignin structures (data not shown but available in Farrell *et al.* 2021). These findings demonstrate that MIR or NIR spectra could also be used to predict the allocation of organic amendment carbon to fast and slow decomposing pools with only a minor reduction in prediction power relative to that obtained with NMR analyses.

## Discussion

Our comprehensive suite of OAs diverse in OC chemistry allowed us to demonstrate that intrinsic decomposability of natural organic matter can be successfully partitioned by spectroscopic techniques ranging from high-end laboratory instrumentation (NMR) through to potentially field-portable technology (NIR). Importantly, spectroscopic discrimination between the amendments was primarily on a chemically meaningful basis, drawing out differences in carbohydrate-, lignin- and protein-like spectroscopic signals.

A wide range of chemical, biological and physical parameters have been proposed to quantify the biological stability of potential soil OAs (Bernal *et al.* 2009; Wichuk and McCartney 2010). In this study, CO<sub>2</sub>-C emission expressed per unit of OAC was measured and used as an index of biological stability. Measures of respiration have been used to quantify OAC stability because, under incubation conditions conducive to optimal decomposition, respiration can provide a direct measure of the OAC availability to decomposer organisms. Goyal *et al.* (2005) found that CO<sub>2</sub>-C emission, along with variations in C/N ratio, provided the most reliable index of compost stability. Bernal *et al.* (1998) measured CO<sub>2</sub>-C emission from four maturation states of seven different composts over a 70 day incubation period. After fitting a combined first-order fast pool and zero-order slow pool to the cumulative CO<sub>2</sub>-C emission data, Bernal *et al.* (1998) found that  $C_f$  and  $C_s$  accounted for 28–489 and 511–972 mg C g<sup>-1</sup> compost C, respectively. The values of  $C_f$  were larger and the values of  $C_s$  were smaller than those derived in this study (0–276 and 723–1000 mg C g<sup>-1</sup> amendment carbon, respectively). Such differences may be attributable to variations in the nature of the materials incubated,

environmental conditions under which the incubations occurred, incubation duration and the model fitted to the data; however, the magnitude of the range in  $C_f$  and  $C_s$  values in this study demonstrates the substantial variation in stability that can exist across different OAs.

In addition to CO<sub>2</sub>-C emission, a range of other parameters including physical (e.g. temperature, particle size, water content), chemical (e.g. C/N ratio, NH<sub>4</sub><sup>+</sup>/NO<sub>3</sub><sup>-</sup> ratio, cation exchange capacity, pH, humification indices) and biological (e.g. microbial biomass, enzyme activity) have been applied to evaluate the potential stability of decomposing organic materials (Bernal *et al.* 2009; Farrell and Jones 2010; Wichuk and McCartney 2010; Higashikawa *et al.* 2014). Baldock (2007) proposed that these parameters could be divided into two groups: (1) those that define whether an organic material will be decomposed and (2) those that influence the rate at which materials are decomposed. Physical parameters were assigned to the latter group since they do not define the potential for decomposition but rather alter the rate at which decomposition processes proceed. In this study, any impacts due to the physical properties of the OAs were reduced by fine grinding.

Understanding the impact of changes in chemical and biological properties fits into the first group of parameters that define whether an organic material will decompose or not and can be assessed by quantifying elemental and biochemical compositional properties. One of the elemental properties often used to characterise the susceptibility of organic materials to decomposition is the C/N ratio (Taylor *et al.* 1989). No relationship was found between initial C/N ratio of the OAs included in this work and the parameters derived to quantify OC mineralisation over the 547 day incubation period used. This result supports the suggestion of Incerti *et al.* (2017) that the reliability of C/N as a decomposability indicator throughout the decomposition process may be questionable as the molecular composition of the organic materials present change as decomposition progresses. A correlation between N content and the predicted decomposition rate constant of the fast pool ( $f$ ) was noted in this study. Although it only accounted for 20% of the variability, similar correlations were noted between  $f$  and the proportion of signal intensity in NMR regions associated with protein (alkyl, N-alkyl and carbonyl). Taken together these suggest some reliance on

the presence of N as protein during the early more rapid phase of decomposition.

Quantification of the impact of biochemical properties is now possible using spectroscopic measurements combined with chemometric techniques. However, even in the absence of chemometric analyses, useful information pertaining to differences in chemical composition existing between OAs or temporal changes that occur as decomposition proceeds can be obtained from spectroscopic analyses. Ait Baddi *et al.* (2004) and Spaccini and Piccolo (2008) interpreted MIR spectra collected from materials exposed to increasing durations of composting to show a loss of labile aliphatic C and an accumulation of aromatic and stable hydrophobic C. Assessment of MIR spectra acquired by Hsu and Lo (1999) over a 122 day composting period was reported to reveal an increase in signal intensity associated with aromaticity and a decrease in signal associated with carbohydrates.

Baldock *et al.* (1997) demonstrated that the ratio of  $^{13}\text{C}$  NMR signal intensity found in the alkyl to O-alkyl chemical shift regions could be used as an index of the degree of decomposition of organic materials and that the absolute values and extent of change showed a dependence on the nature of the initial material. Similar results were obtained by Preston *et al.* (2009) on characterising litter from 6-year field incubation studies. Incerti *et al.* (2017) developed a modelling framework that used the allocation of  $^{13}\text{C}$  NMR signal intensity to chemical shift ranges within the alkyl, N-alkyl, O-alkyl and di-O-alkyl shift regions to enhance the prediction of decomposition rates.

Although the information gained from spectra alone is informative, it is difficult to (1) quantify the magnitude of structural change, (2) extract all relevant information from spectra, particularly in complex spectral regions where signal intensity can be derived from multiple sources and (3) define the relationship between spectral data and analytical data. Coupling spectroscopic data with analytical data through chemometric analyses can be used to develop predictive capabilities. Higashikawa *et al.* (2014) measured a range of compost maturity indices for 15 different composts and then successfully built a series of MIR/PLSR predictive models for the indices to allow the prediction of all indices from one MIR spectrum. Similar results were obtained by Vergnoux *et al.* (2009) and Lillhonga *et al.* (2009) using NIR/PLSR to predict a series of stability parameters measured temporally on composts. Martínez-Sabater *et al.* (2009) used a combination of  $^{13}\text{C}$  NMR and MIR with multivariate analyses to quantify temporal changes in the chemical composition of composts and develop predictive algorithms defining composting time as a function of whole spectra or spectral components. Bonanomi *et al.* (2013) coupled measured decay rates from a litter bag experiment with acquired  $^{13}\text{C}$  NMR spectra through principal component regression analysis to build a predictive litter decomposition algorithm. Thus, it is apparent that spectroscopy coupled with chemometric analysis shows promise to predict stability, and therefore also C loss from OAs such as those studied here.

In this study, chemometric analyses (PCA and PLSR) were applied to NMR, MIR and NIR spectra to define differences in

chemical composition across a series of 85 different soil OAs and to predict the allocation of amendment carbon to fast and slow decomposing pools. In the application of PCA to the NMR spectra, in addition to identifying which amendments had different chemical compositions based on an examination of the scores plot (Fig. 4b) the loadings spectra (Fig. 4c) could be used to identify the chemical changes associated changes in positioning on the scores plot. When the loadings spectra were compared with NMR spectra acquired for known biomolecules, the compositional differences responsible for influencing PC-1 scores (a positive contribution from carbohydrate and a negative contribution from protein) and PC-2 scores (a positive contribution from lignin and negative contributions from protein and carbohydrate) became evident. Taking a similar approach in the PLSR analyses by examining the  $\beta$ -coefficient spectra (Fig. 7b, d, f and h) contributed to understanding why different allocations of amendment carbon to  $C_f$  and  $C_s$  were obtained ( $C_f$  increased as the allocation to protein and carbohydrate C increased and decreased as in response to an increasing contribution of lignin). The usefulness of these loading and  $\beta$ -coefficient spectra in helping to explain the reasons behind separation of amendments in PCA space and the prediction of  $C_f$  by PLSR algorithms do not appear to have been reported previously.

Despite success across all three spectral techniques in predicting the partitioning of OAC to labile ( $C_f$ ) and more resistant ( $C_s$ ) pools, predicting the magnitude of the rate constants associated with the mineralisation of C from these pools ( $f$  and  $s$ , respectively) was not successful. In soils, decomposition of OC may be constrained through protection of the OC by sorption to clay particles (Schmidt *et al.* 2011) or occlusion within aggregate structures (Dungait *et al.* 2012). By using only minimal soil within our sand matrix, we sought to avoid these factors which obscure the intrinsic decomposability of a substrate and thus the relationship back to its chemical composition. These, and other factors (such as temperature and oxygen, water, and nutrient availability, as well as the composition of the microbial community) modify these decomposition rate constants (Jenkinson 1990; Gregorich *et al.* 2017). Although we normalised for water and oxygen availability, temperature, starting microbial community composition and the potential for protection from decomposition through our experimental design, they were not properties that would be expressed in a spectral analysis of the amendments. This is particularly true for NMR, which in the configuration used here only detected chemically different forms of OC but yet gave the most accurate predictions of pool size.

## Conclusions

The best PLSR algorithms for predicting whether OAC was associated with a pool or C exhibiting in a fast ( $C_f$ ) or slow ( $C_s$ ) susceptibility to mineralisation were obtained using the NMR spectra. Decreases in predictive capability (reductions in  $R^2$  and RMSE values) using MIR and NIR spectra were minor. Therefore, with adequate calibration, rapid and cost-effective predictions of the allocation of OAC to fast and slow

decomposing pools based on MIR or NIR should be possible. However, given our inability to accurately predict rate constants with any of the spectroscopy techniques used here, prediction of expected residence time upon application to soil would likely require information on soil, environmental and management properties at the site of application. Nevertheless, deployment of field portable NIR spectrometers, backed by appropriate calibrations, would allow OA producers to quickly and cost effectively monitor and manage composition to provide products that are appropriately matched to desired outcomes.

### Conflict of interest

Mark Farrell is Guest Editor of the Soil Organic Matter in a Stressed World Special Issue and is an Associate Editor for *Soil Research*. He had no editorial involvement with this paper, which was handled independently by other members of the Editorial Board. The authors declare no real or apparent conflicts of interest.

### Acknowledgements

We thank the Australian Government for funding under the Filling the Research Gap Program. Bruce Hawke is thanked for the MIR and NIR analysis.

### References

- Adair E, Parton W, Del Grosso S (2008) Simple three-pool model accurately describes patterns of long-term litter decomposition in diverse climates. *Global Change Biology* **14**, 2636–2660. doi:10.1111/j.1365-2486.2008.01674.x
- Ait Baddi G, Antonio Alburquerque J, González J, Cegarra J, Hafidi M (2004) Chemical and spectroscopic analyses of organic matter transformations during composting of olive mill wastes. *International Biodeterioration & Biodegradation* **54**, 39–44. doi:10.1016/j.ibiod.2003.12.004
- Baldock JA (2007) Composition and cycling of organic carbon in soil. In 'Soil Biology, Volume 10. Nutrient Cycling in Terrestrial Ecosystems'. (Eds P Marschner, Z Rengel.) pp. 1–35. (Springer-Verlag: Berlin).
- Baldock JA, Smernik RJ (2002) Chemical composition and bioavailability of thermally altered *Pinus resinosa* (Red pine) wood. *Organic Geochemistry* **33**, 1093–1109. doi:10.1016/S0146-6380(02)00062-1
- Baldock JA, Oades JM, Nelson PN, Skene TM, Golchin A, Clarke P (1997) Assessing the extent of decomposition of natural organic materials using solid-state <sup>13</sup>C NMR spectroscopy. *Australian Journal of Soil Research* **35**, 1061–1084. doi:10.1071/S97004
- Baldock JA, Wheeler I, McKenzie N, McBratney A (2012) Soils and climate change: potential impacts on carbon stocks and greenhouse gas emissions, and future research for Australian agriculture. *Crop and Pasture Science* **63**, 269–283. doi:10.1071/CP11170
- Baldock J, Hawke B, Sanderman J, Macdonald L (2013a) Predicting contents of carbon and its component fractions in Australian soils from diffuse reflectance mid-infrared spectra. *Soil Research* **51**, 577–595. doi:10.1071/SR13077
- Baldock J, Sanderman J, Macdonald L, Massis A, Hawke B, Szarvas S, McGowan J (2013b) Quantifying the allocation of soil organic carbon to biologically significant fractions. *Soil Research* **51**, 561–576. doi:10.1071/SR12374
- Bernal MP, Sánchez-Monedero MA, Paredes C, Roig A (1998) Carbon mineralization from organic wastes at different composting stages during their incubation with soil. *Agriculture, Ecosystems & Environment* **69**, 175–189. doi:10.1016/S0167-8809(98)00106-6
- Bernal MP, Alburquerque JA, Moral R (2009) Composting of animal manures and chemical criteria for compost maturity assessment. A review. *Bioresource Technology* **100**, 5444–5453. doi:10.1016/j.biortech.2008.11.027doi:19119002
- Bonanomi G, Incerti G, Giannino F, Mingo A, Lanzotti V, Mazzoleni S (2013) Litter quality assessed by solid state <sup>13</sup>C NMR spectroscopy predicts decay rate better than C/N and lignin/N ratios. *Soil Biology & Biochemistry* **56**, 40–48. doi:10.1016/j.soilbio.2012.03.003
- Dalal RC, Wang WJ, Robertson GP, Parton WJ (2003) Nitrous oxide emission from Australian agricultural lands and mitigation options: a review. *Australian Journal of Soil Research* **41**, 165–195. doi:10.1071/SR02064
- de Freitas Maia C, Novotny E, Rittl T, Hayes M (2013) Soil organic matter: chemical and physical characteristics and analytical methods. A review. *Current Organic Chemistry* **17**, 2985–2990. doi:10.2174/13852728113179990123
- Dungait JAJ, Hopkins DW, Gregory AS, Whitmore AP (2012) Soil organic matter turnover is governed by accessibility not recalcitrance. *Global Change Biology* **18**, 1781–1796. doi:10.1111/j.1365-2486.2012.02665.x
- Farrell M, Jones DL (2010) Food waste composting: Its use as a peat replacement. *Waste Management* **30**, 1495–1501. doi:10.1016/j.wasman.2010.01.032doi:20185289
- Farrell M, Baldock J, Creamer C, Szarvas S, McGowan J, Carter T (2021) Spectral chemistry and decomposition characteristics of a range of organic amendments. v1. CSIRO Data Collection. doi:10.25919/hj7a-h494. doi:10.25919/hj7a-h494
- Glanville HC, Hill PW, Schnepf A, Oburger E, Jones DL (2016) Combined use of empirical data and mathematical modelling to better estimate the microbial turnover of isotopically labelled carbon substrates in soil. *Soil Biology & Biochemistry* **94**, 154–168. doi:10.1016/j.soilbio.2015.11.016
- Goyal S, Dhull SK, Kapoor KK (2005) Chemical and biological changes during composting of different organic wastes and assessment of compost maturity. *Bioresource Technology* **96**, 1584–1591. doi:10.1016/j.biortech.2004.12.012doi:15978991
- Gregorich EG, Janzen H, Ellert BH, Helgason BL, Qian B, Zebarth BJ, Angers DA, Beyaert RP, Drury CF, Duguid SD, May WE, McConkey BG, Dyck MF (2017) Litter decay controlled by temperature, not soil properties, affecting future soil carbon. *Global Change Biology* **23**, 1725–1734. doi:10.1111/gcb.13502doi:27633488
- Guenet B, Gabrielle B, Chenu C, Arrouays D, Balesdent J, Bernoux M, Bruni E, Caliman J-P, Cardinael R, Chen S, Ciais P, Desbois D, Fouche J, Frank S, Henault C, Lugato E, Naipal V, Nesme T, Obersteiner M, Pellerin S, Powelson DS, Rasse DP, Rees F, Soussana J-F, Su Y, Tian H, Valin H, Zhou F (2021) Can N<sub>2</sub>O emissions offset the benefits from soil organic carbon storage? *Global Change Biology* **27**, 237–256. doi:10.1111/gcb.15342doi:32894815
- Hénault C, Gossel A, Mary B, Rousset M, Léonard J (2012) Nitrous oxide emission by agricultural soils: A review of spatial and temporal variability for mitigation. *Pedosphere* **22**, 426–433. doi:10.1016/S1002-0160(12)60029-0
- Higashikawa FS, Silva CA, Nunes CA, Sánchez-Monedero MA (2014) Fourier transform infrared spectroscopy and partial least square regression for the prediction of substrate maturity indexes. *The Science of the Total Environment* **470–471**, 536–542. doi:10.1016/j.scitotenv.2013.09.065doi:24176701
- Hoyle FC, Baldock JA, Murphy DV (2011) Soil organic carbon - role in rainfed farming systems: with particular reference to Australian conditions. In 'Rainfed Farming Systems'. (Eds P Tow, I Cooper, I Partridge, C Birch.) pp. 339–361. (Springer Science: Berlin).
- Hsu JH, Lo SL (1999) Chemical and spectroscopic analysis of organic matter transformations during composting of pig manure. *Environmental Pollution* **104**, 189–196. doi:10.1016/S0269-7491(98)00193-6

- Incerti G, Bonanomi G, Giannino F, Carteni F, Spaccini R, Mazzei P, Piccolo A, Mazzoleni S (2017) OMDY: a new model of organic matter decomposition based on biomolecular content as assessed by  $^{13}\text{C}$ -CPMAS-NMR. *Plant and Soil* **411**, 377–394. doi:10.1007/s11104-016-3039-2
- Jenkinson DS (1990) The turnover of organic carbon and nitrogen in soil. *Philosophical Transactions of the Royal Society of London. Series B, Biological Sciences* **329**, 361–368. doi:10.1098/rstb.1990.0177
- Johnston AE, Poulton PR, Coleman K (2009) Chapter 1 Soil Organic Matter: Its Importance in Sustainable Agriculture and Carbon Dioxide Fluxes. In 'Advances in Agronomy'. (Ed. DL Sparks.) Vol. 101, pp. 1–57. (Academic Press: Cambridge).
- Kalbitz K, Schmerwitz J, Schwesig D, Matzner E (2003) Biodegradation of soil-derived dissolved organic matter as related to its properties. *Geoderma* **113**, 273–291. doi:10.1016/S0016-7061(02)00365-8
- Lillhonga T, Grunwald J, Geladi P (2009) Chemometric monitoring of designed composting processes using laboratory measurements and near infrared spectroscopy. *Journal of Near Infrared Spectroscopy* **17**, 275–287. doi:10.1255/jnirs.852
- Macdonald L, Farrell M, Baldock J (2016) The influence of increasing organic matter content on  $\text{N}_2\text{O}$  emissions. In 'Proceedings of the 2016 International Nitrogen Initiative Conference, Solutions to improve nitrogen use efficiency for the world', 4–8 December 2016, Melbourne, Australia. (International Nitrogen Initiative)
- Manlay RJ, Feller C, Swift MJ (2007) Historical evolution of soil organic matter concepts and their relationships with the fertility and sustainability of cropping systems. *Agriculture, Ecosystems & Environment* **119**, 217–233. doi:10.1016/j.agee.2006.07.011
- Martínez-Sabater E, Bustamante MA, Marhuenda-Egea FC, El-Khattabi M, Moral R, Lorenzo E, Paredes C, Gálvez LN, Jordá JD (2009) Study of the evolution of organic matter during composting of winery and distillery residues by classical and chemometric analysis. *Journal of Agricultural and Food Chemistry* **57**, 9613–9623. doi:10.1021/jf901027vdoi:19795879
- Melillo JM, Aber JD, Muratore JF (1982) Nitrogen and lignin control of hardwood leaf litter decomposition dynamics. *Ecology* **63**, 621–626. doi:10.2307/1936780
- Paul EA, Clark FE (1996) 'Soil Microbiology and Biochemistry, Second Edition.' (Academic Press: Cambridge).
- Paustian K, Collins HP, Paul EA (1997) Management controls on soil carbon. In 'Soil Organic Matter in Temperate Agroecosystems. Longterm Experiments in North America'. (Eds EA Paul, ET Elliott, K Paustian, CV Cole.) pp. 15–49. (CRC Press: Boca Raton, FL, USA)
- Preston CM, Nault JR, Trofymow JA (2009) Chemical changes during 6 years of decomposition of 11 litters in some Canadian forest sites. Part 2.  $^{13}\text{C}$  abundance, solid-state  $^{13}\text{C}$  NMR spectroscopy and the meaning of "lignin". *Ecosystems* **12**, 1078–1102. doi:10.1007/s10021-009-9267-z
- R Core Team (2020). R: A language and environment for statistical computing. R Foundation for Statistical Computing, Vienna, Austria. URL. Available at <https://www.R-project.org/>.
- Rayment, GE, Lyons, DJ (2011) Soil chemical methods – Australasia. (CSIRO publishing: Melbourne).
- Reeves DW (1997) The role of soil organic matter in maintaining soil quality in continuous cropping systems. *Soil & Tillage Research* **43**, 131–167. doi:10.1016/S0167-1987(97)00038-X
- Rynk R (2003) The art in the science of compost maturity. *Compost Science & Utilization* **11**, 94–95. doi:10.1080/1065657X.2003.10702116
- Sanderman J, Creamer C, Baisden WT, Farrell M, Fallon S (2017) Greater soil carbon stocks and faster turnover rates with increasing agricultural productivity. *Soil (Göttingen)* **3**, 1–16. doi:10.5194/soil-3-1-2017
- Schmidt MWI, Torn MS, Abiven S, Dittmar T, Guggenberger G, Janssens IA, Kleber M, Kogel-Knabner I, Lehmann J, Manning DAC, Nannipieri P, Rasse DP, Weiner S, Trumbore SE (2011) Persistence of soil organic matter as an ecosystem property. *Nature* **478**, 49–56. doi:10.1038/nature10386doi:21979045
- Shukla MK, Lal R, Ebinger M (2006) Determining soil quality indicators by factor analysis. *Soil & Tillage Research* **87**, 194–204. doi:10.1016/j.still.2005.03.011
- Spaccini R, Piccolo A (2008) Spectroscopic characterization of compost at different maturity stages. *CLEAN – Soil, Air Water (Basel)* **36**, 152–157.
- Taylor BR, Parkinson D, Parsons WFJ (1989) Nitrogen and lignin content as predictors of litter decay rates: a microcosm test. *Ecology* **70**, 97–104. doi:10.2307/1938416
- Thuriès L, Pansu M, Larré-Larrouy MC, Feller C (2002) Biochemical composition and mineralization kinetics of organic inputs in a sandy soil. *Soil Biology & Biochemistry* **34**, 239–250. doi:10.1016/S0038-0717(01)00178-X
- Vergnoux A, Guiliano M, Le Dréau Y, Kister J, Dupuy N, Doumenq P (2009) Monitoring of the evolution of an industrial compost and prediction of some compost properties by NIR spectroscopy. *The Science of the Total Environment* **407**, 2390–2403. doi:10.1016/j.scitotenv.2008.12.033doi:19167742
- Walela C, Daniel H, Wilson B, Lockwood P, Cowie A, Harden S (2014) The initial lignin:Nitrogen ratio of litter from above and below ground sources strongly and negatively influenced decay rates of slowly decomposing litter carbon pools. *Soil Biology & Biochemistry* **77**, 268–275. doi:10.1016/j.soilbio.2014.06.013
- Wei T, Simko V (2017). R package 'corrplot': Visualization of a Correlation Matrix (Version 0.84). Available from <https://github.com/taiyun/corrplot>.
- Wichuk KM, McCartney D (2010) Compost stability and maturity evaluation - a literature review. *Canadian Journal of Civil Engineering* **37**, 1505–1523. doi:10.1139/L10-101
- Wickham H, Averick M, Bryan J et al. (2019) Welcome to the tidyverse. *Journal of Open Source Software* **4**, 1686. doi:10.21105/joss.01686

Handling Editor: Mark Tibbett